Fire resistance of axial restraint composite floor steel cellular beams

Ali Nadjai[a, *]

a.nadjai@ulster.ac.uk

Sanghoon Han[a]

s.han@ulster.ac.uk

Faris Ali[a]

f.ali@ulster.ac.uk

Naveed Alam[a]

alam-n1@ulster.ac.uk

Ahmed Allam[b]

[a]University of Ulster, FireSERT, Dept. of Built Environment, UK

[b]International Fire Consultants Group (IFC), UK

*Corresponding author.

ABSTRACTbstract

In a fire situation, axial restraint force can threaten the structural performance, but these influences do not appear in an isolated beam's furnace test. With this issue, the authors introduced an outer frame around the furnace to give a pin-end supports and axial restraint stiffness which can be controlled to set various restraint factors on the fire tested beam specimen. This paper presents three fire tests conducted on full scale composite Cellular Beams (CB) with different slab decking shapes subjected to vertical loading and axial restraint effect. As a result, temperatures, deflections, strain and displacement and failure mode are discussed to assess actual behaviour of the composite CB and compared with previous CB tests series which were conducted by the University of Ulster.

1.1 Introduction

Cellular beams (CBs) are currently being widely used in multi-storey buildings which reduce the total weight of steelwork and help to decrease the floor depth by accommodating pipes, conduits and ducting within web openings. They are also used in commercial and industrial buildings, warehouses, and portal frames. CBs, produced by modern automated fabrication processes can be competitive for the construction of both floor and roof systems. Their widespread use as structural members has prompted several investigations into their structural behaviour. When subjected to fire, the steel and composite structures will lose their loading capacity and stiffness. To ensure the safety of life and properties of public, the indispensable fire resistance of the building is required by the authority [1]. Traditionally, fire resistance ability of the structural members was tested using the isolated element heated against the ISO standard fire. In this methodology, the buildings were treated as a series of individual members while the continuities and interaction between these members were assumed to be negligible. Consequently, most of the structural steel members need to be protected by insulation materials, such as intumescent paints and fire protection boards, to achieve the required fire resistance. Throughout the 1990s, following the investigation of the fire event in Broadgate [2], fire tests in William Street [3], full-scale fire tests on a 8-storey composite steel-framed building in Cardington [4,5] and recently fire compartment of longer cellular beams in fire [6], it was found that the structural members in the frame had a significantly better behaviorbehaviour in fire than that in the standard fire resistance test. The standard fire test was very conservative by disregarding the interaction between members. The fire event and tests also highlighted that the current Codes, although conservative, were not addressing the true behaviorbehaviour of building structure in fire, since the building was not acting as a series of individual members [5,7].

However, in a continuous structure, the steel elements, including beams, are usually under axial restraint from adjacent structure. In a fire situation, relatively cool adjacent members, and particularly continuous floor slabs, apply significant restraint to the ends of a beam which is expanding at high temperatures. This restraint creates axial compression forces for which the beam has not been designed, and which could threaten its structural

performance, introducing the possibility of lateral-torsional and distortional buckling. Recently research [8–11] have clearly shown that the axial restraint has significantly influenced on the fire response of restrained solid beams.

At the University of Ulster FireSERT, several simply supported cellular beams were tested in fire conditions [12,13] and other [14] but with no consideration of the axial effects. With funding from the EPSRC: EP/F001525/1 the state-of-the-art combustion chamber at Ulster, 5 m × 3 m in plan × 3 m in height which was extended to accommodate longer spans of 6.7 m, complete with reaction frames for loading and restraint, instrumentation and control equipment were used in the experimental study (see Figures 1 and 2). The additional reaction frame constructed around the furnace is capable of applying axial restraint stiffness to give an additional flexibility and thus change the restraint ratio. All beams will have pin-ended supports to enable the measurement of the generated forces. The support of the hinge will allow two-way axial restraint-spring mechanisms to be applied. This means that the axial restraint will be imposed during expansion and contraction stages. The two-way mechanism will ensure more realistic simulation of axial restraint.

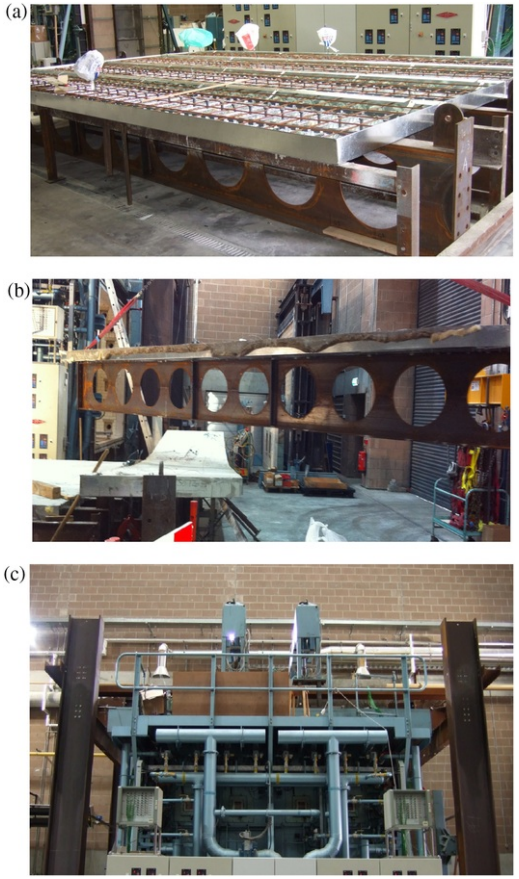

Fig. 1 Test preparation: a) composite beams; b) specimen ready for test; c) large furnace.

alt-text: Fig. 1

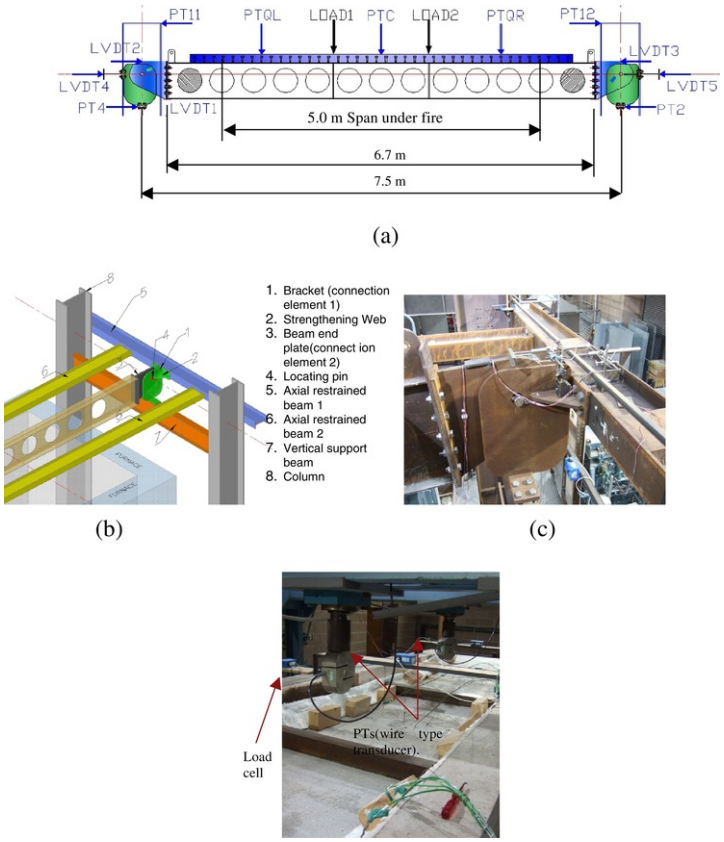

Fig. 2 Composite floor detailing: a) specimen elevation view, b) detailing of pin joint, c) restraint pin joint photo.

alt-text: Fig. 2

~~2.~~2 Experimental set up

This study consisted of an experimental programme (Table 1) on three full scales symmetric composite floor unprotected cellular beams with axially restrained pin-end conditions having different decking systems, slab thickness and shear connectors (Fig~~ure~~. 2). The symmetrical cellular beam was produced based on UB 406 × 140 × 39 (S355) as a top and bottom tee section having a finished depth of CB571 × 140 × 39 kg/m. Distance between the supports with end plate is 7.5 m and the diameter of cell is 375 mm with 500 mm centre spacing.

Table 1 Geometry data of steel section (Beam 1, Beam 2 and Beam 3).

alt-text: Table 1

Flange width(mm)	141.8 (top)	141.8 (bottom)		
Flange thickness (mm)	8.6 (top)	8.6 (bottom)		
Web thickness (mm)	6.4 (top)	6.4 (bottom)		
Cell details (mm)	500 (spacing)	375 (diameter)		
Depth (mm)	285.5 (top)	285.5 (bottom)	571 (overall)	

Number of cells	11 (circular)	0 (elongated)	2 (infill)	0 (semi-infill)

~~2.1.~~2.1 Composite concrete slab

Overall composite slab (Fig~~ures~~. 3 and 4) thickness was 130 mm for the Beam 1, Beam 2 and 120 mm for Beam 3 (from the bottom of the rib of the profiled steel sheeting to the outer face of the concrete slab) with 1100 mm width and 6000 mm in length constructed using normal-weight concrete (Grade C35). The slab includes a welded A393 Steel Reinforcing mesh having a total length of 1000 mm with a yield strength of 460 N/mm^2.This mesh is made with wires of ø10 mm diameter and with 200 ~~x~~ × 200 mm spacing. This mesh is overlaid with 40 mm of concrete during the construction. The double shear connectors in Beam 1 are staggered equally at 323 mm from each other. In case of Beam 2 and Beam 3, single headed studs, equally distributed at 150 mm over the beam length have been provided. The shear connectors are ø19 mm in diameter and are 95 mm in length to ensure a full interaction between the slab and the cellular beam for all three cases.

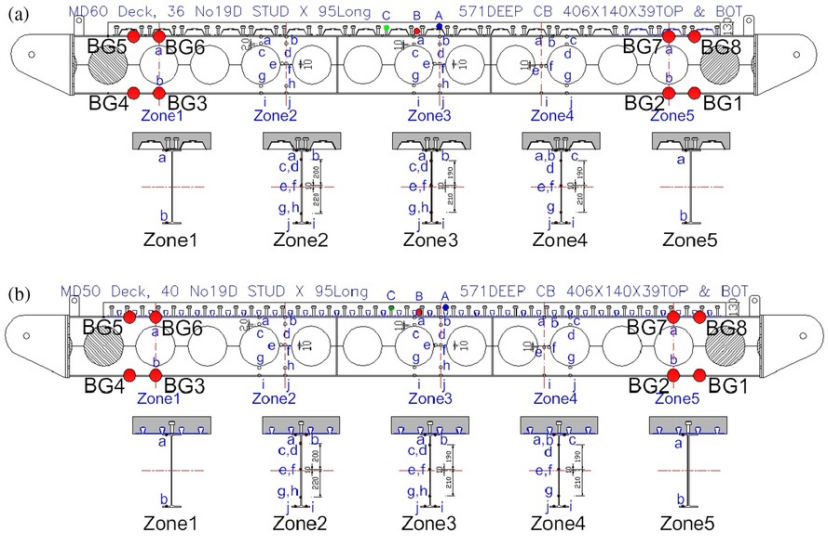

Fig. 3 Composite cellular beam and TC location through the section a) Beam 1; b) Beam 2 and Beam 3 are similar except slab thickness is different.

alt-text: Fig. 3

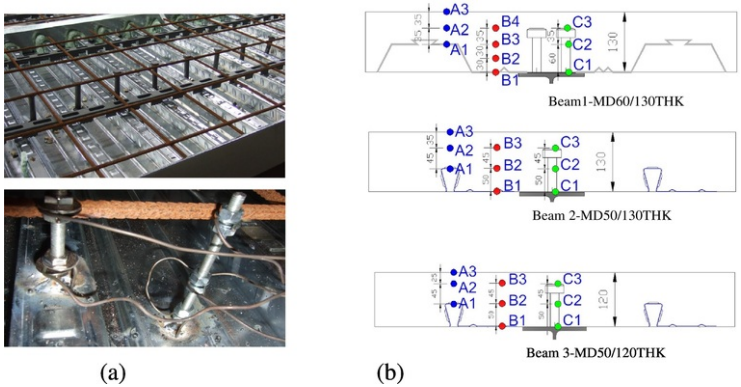

Fig. 4 ~~-~~Slab thermocouple~~-~~ locations: a) decking photo, b) detailing positions.

alt-text: Fig. 4

2.2.2.2 Profiled steel sheeting

The steel deck was Multideck 60-V2 (Kingspan MD60) for Beam 1 and MD50 for Beam 2 and Beam 3 with strength 350 N/mm^2 and thickness 0.9 mm. The Steel strip complies with BS EN 10143 [15] and BS EN 10147 [16] with minimum yield strength of 350 N/mm^2 and a minimum coating mass of 275 g/m^2.

2.3.2.3 Details of outer restrain frame

Support conditions were designed with pin-end (Figure. 2) and axial restraint stiffness (figure) to represent the effect of surrounding structures. Two of 305 × 165 × 54UB and two of 305 × 127 × 48UB were used for lateral and longitudinal directions outer frame respectively along the test beam specimen. The latter members were 8136 mm long and placed with 2010 mm of centre to centre spacing. The plan, side elevation, detailing of the connections for the restraint frame as well as the experimental set up are all shown in Figure. 2. The restrain stiffness was calculated as 7.06 kN/mm from the STAAD Pro-QSE software simulation and it also approached by the overall equivalent stiffness concept (Eq. 1) for the neighbouring system.

$$K = \frac{1}{\left(\frac{1}{k_1} + \frac{1}{k_2} + \frac{1}{k_3} + \ldots\right)} \quad \textbf{(1)}$$

where:

K is the total axial stiffness of outer frame,

k_n is the stiffness of each member to the global axial direction.

The axial stiffness of composite CB was assumed from Eurocode and SCI guidance [17] to get restrain factor (restraint stiffness to the axial stiffness of the specimen beam, Table 2) for this experimental program.

Table 2 Load ratio and restrain factor.

alt-text: Table 2

	Moment capacity	Applied load	Applied moment	Load ratio	Restrain factor
Beam 1	478.37 kN m	90 kN	135 kN m	0.282	0.12
Beam 2 & 3	481.84 kN m	90 kN	135 kN m	0.280	0.11

2.4.2.4 Mechanic loading

Two concentrated loads (Figure. 2), symmetric about mid-span (1.5 m distance of 2 loads), were used for the beam test. The applications of hydraulic pressure were equal to 90 kN for Beam 1, 2 and 3. Load applied was around 30% of the ultimate load found from the pre-design at cold conditions and by taken into account from the previous tests conducted at Ulster University as reference [13]. Pre-loading tests were also conducted on the pure steel CBs before concrete casting for the calibration of steel beam and outer frame behaviour and that of the measuring device. Before the application of full loading on the composite beam, half of target pressure as a pre-loading was applied for settlement on the reaction frame. The axial restraint on the test beam was addressed through the outer frame. Table 2 shows applied load ratio and restrain factor.

2.5.2.5 Test measurements

Temperature profiles along the beam and across the web-posts, top and bottom flanges were measured using 1 mm sheathed Type K thermocouples (Figure. 3). Temperature measurements were taken on the exposed and unexposed slab surfaces and at its mid-height, at several locations including shear studs (Figfigure. 4). Deflections of test beam and displacements of frame elements were recorded using LVDTs and PTs (wire type transducer) as it is illustrated in Figure. 5. For the strain measurements on steel beam (cold area), outer beam and concrete slab, a number of strain gages were applied. An illustration of this is given in Figuress. 3 and 5a.

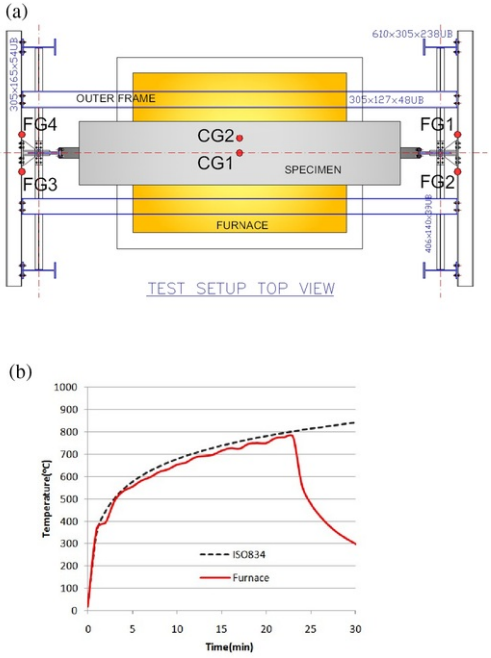

~~Figure 5~~Fig. 5 Average temperature of the furnace (Test beam 2).

alt-text: Fig. 5

~~2.6.~~2.6 Furnace temperature

Eight thermocouples were inserted through the side walls of combustion chamber of the furnace to control the heating conditions and to assess if the ISO parametric fire curve was followed as shown in Figure 5b. Only the lower side of the slab and 3 sides of the steel section were fire-exposed.

The following function (Eq. 2) represents the ISO fire curve:

$$T = 345\log_{10}(8t + 1) + 20 \quad \textbf{(2)}$$

where: t is the time (min).

~~3.~~3 Test results and analysis

~~3.1.~~3.1 Temperature distribution

Figure 6 shows typical variations against time of the temperatures at the bottom of flange, web, top flange, and slab at mid span of the three composite cellular steel beams during the heating and cooling phases. The heat absorbed by the three beams show that the highest temperatures recorded were in the middle of the webs up to 15 ~~minutes~~min with a little difference compared to the bottom flanges but it becomes similar after 20 ~~minutes~~min heating time. The difference between the web and top flange temperatures for Beam 2 and 3 increased to almost 300 ~~o~~°C after 10 ~~minutes~~min except for Beam 1 where an increase of 120 ~~o~~°C was recorded. This is due to the top flange being exposed to heat compared to Beams 2 and 3 as the decking shape create different surrounding conditions. The maximum temperature values of steel section were recorded in the bottom tee, reaching up to 730~~o~~ °C after 20 ~~minutes~~min in all beams.

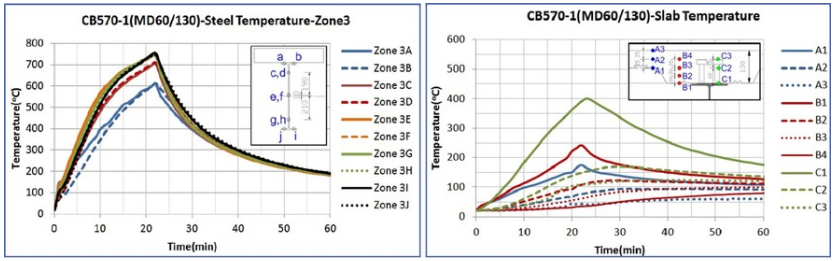

(a)

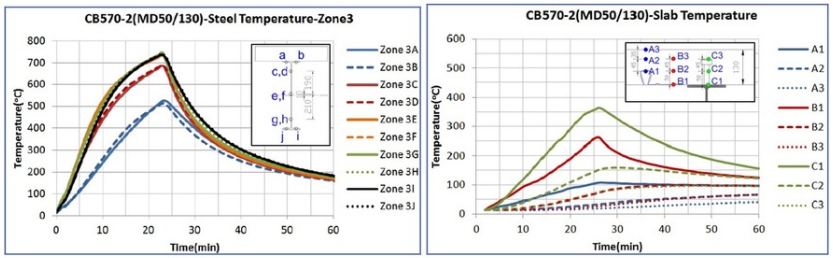

(b)

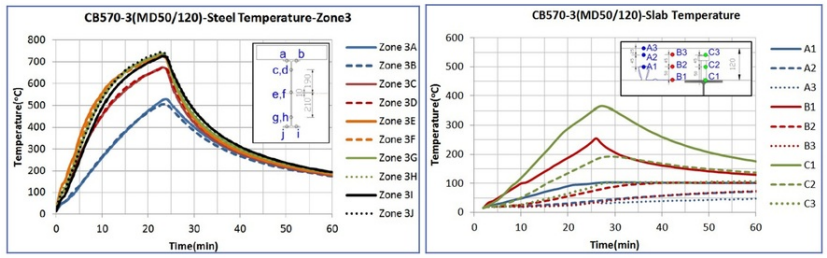

(c)

Fig. 6 Steel temperature (Zone 3) and slab temperature (A–C) a) Beam 1; b) Beam 2, c) Beam 3.

alt-text: Fig. 6

Fig~~ure~~. 6 demonstrated that temperature on the concrete slab was also affected by the volume of concrete and decking shape as the rising temperature of concrete and shear stud are different in same time. After the results obtained from 20 ~~minutes~~min fire exposure, it can be concluded that the Cellular steel beams lost strength but the temperatures in the slab thickness kept the steel reinforcement cooler about 200 ~~o~~°C lesser. The steel reinforcement, being at a lower temperature becomes effective with the shear connectors and the beams behaves as a reinforced concrete slab with the load being resisted by the bending action. Catenary action may then develop with the reinforcement acting in direct tension rather than bending. It can also been seen in Fig~~ure~~. 6 that heating of the specimens is discontinued after around 23 ~~minutes~~min as at this point, ~~behavior~~behaviour of the beam changed due to catenary action and hence the beam was allowed to cool down at its own. The main purpose to avoid further heating was due to the loss of stiffness of the beam as it started to behave as a cable at this point. Thermal recordings were continued till 60 ~~minutes~~min from the start of the experiment. Temperatures recordings were also continued for in the slab during the cooling phase.

It can also be seen in Fig~~ure~~. 6 that the decking type has an influence on the temperature distributions in slab and in the shear connectors. In case of Beam 1, the decking shape resulted in higher fire exposure area which resulted in higher temperature recordings as compared to those obtained from Beam 2 and Beam 3. Further, depth of the slab in case of Beam 2 and Beam 3 has very less effect on the temperatures recorded.

~~3.2.~~3.2 Structure behaviour

~~3.2.1.~~*3.2.1 Deflection*

Figure 7 show the temperature – deflection curves for Beam 1 and Beam 2. Both beams were able to sustain the load without excessive deflection up to web post time is 10 minutesmin with a recording temperature of about 550 °C. Further rise in temperature led to web post buckling followed by progressive run away of the cellular beams in vertical deflection as the loss of stiffness and strength accelerated. It can be seen in Figure 7 that vertical deflection for Beam 1 and Beam 2 exceeded the limits after 22 and 23 minutesmin of heating respectively. From this point onwards, as no further heating was done and the beam was allowed to cool, hence, the direction of deflection changed and some recovery was observed. Though the temperatures were recorded for 60 minutesmin from the start of test, however, deflections were not recorded beyond 25 minutesmin as the beam specimens have already exceeded the deflection limits resulting in failure.

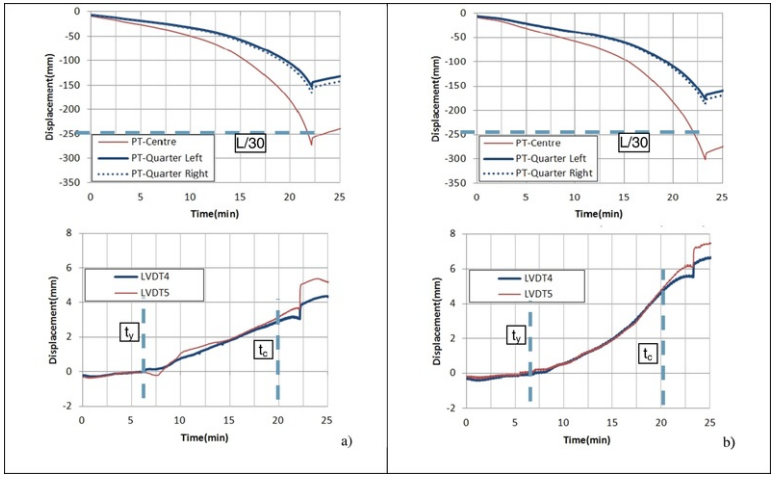

Fig. 7 Vertical deflection (PTs) and outer frame lateral displacement(LVDT4-5) a) Beam 1; b) Beam 2.

alt-text: Fig. 7

As the deflection in case of Beam 1 and Beam 2 is same, hence, it could be the result of the double shear connectors in the prior case as it compensates for the lesser effective depth of the slab resulting from the decking shape. In addition, it seems that in these composite beams with down-stand steel sections, the slab itself has lesser influence on the deflection if proper shear connection is provided.

3.2.2.3.2.2 *Axial effect*

From Figure 7, the vertical deflections of both cellular beams are quite similar but the axial displacements creating axial compression force is more in beam 2 and this due to the slab thickness and the steel decking shape.

Thermal expansion induced bowing deflection (Eq. 3) took place at the very first stage (up to 400 °C) from the temperature increasing under the constant mechanic loading.

$$\delta_t = \alpha \Delta T L^2 / 8d \quad \textbf{(3)}$$

where

α is the coefficient of thermal expansion

ΔT is the temperature difference between the top and bottom of the beam

d is the height of the cross section.

The next meaningful movement observed at time t_y in Figure 7 (450 °C on the web temperature in 8 minutesmin) was showing a start point of rapid displacement and strain growth that indicates stress on outer frame was increasing due to the occurrence of possible structural yield in the beam (Figure 8). This indicates that during heating, the effects of axial restraint on heated beams should be considered. Figure 7 demonstrates that from 20 °C to 450 °C, the beam changes its response from elastic to plastic while the top flange undergoes compression to tension. At 450 °C, the maximum compressive stress is achieved accompanied with the ultimate value of the internal axial force. At the later heating stage (Figure 8), the whole section is in tension resulting from catenary action.

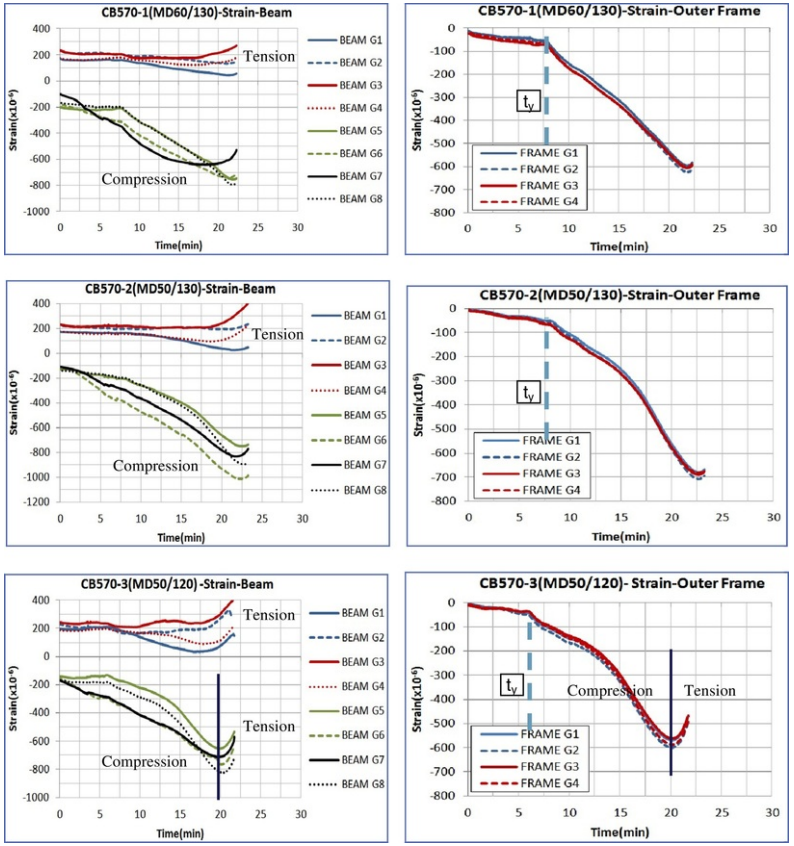

Fig. 8 Restrained beams strain (BG1-8) and outer frame strain (FG1-8).

alt-text: Fig. 8

At time t_c in Figure 7 (720°C temperature on the web in 22 minutes min). The mid-span deflection reached at $L/30$ (250 mm) which regarded a range of the deflection limit state, followed by large deflection as well as changing direction of the frame's axial strain (Figure 8). This could be a sign of the catenary action stage. Thus, in application of catenary action in design, careful examinations of the end conditions and stiffness of adjoining structures are necessary.

Figure 8 shows the developments of different strain rates in the top and bottom flanges at the restraint parts of the beams (see Figure 3) and the restrained frame. At the initial stages of heating, the thermal ε_{th} and mechanical strain rate ε_m govern the total strain rate ε_{tot}, however, beyond the 450 °C, it is expected that the strain rate will be higher. At the point where catenary action developed, strain rates were the highest, but soon after, as the beam started to behave as a cable and strain rates changed their direction. Like in case of vertical and horizontal deflections, no strain rates were recorded during the cooling phase as there was neither heat being applied to the beam nor it was taking any load as it lost its stiffness and connection with the load source.

3.2.3.3.2.3 *Failure mechanism*

Between these two timings, t_y and t_c, there was a development of failure mechanism, combined with a web post buckling and an axial compression under the restrain stiffness. The critical temperature, in the EN, with the load ratio of 0.28 presented as 674 °C on steel section. This critical temperature is specific to steel section only and cannot be applied to CB nor to composite structure as the failure mechanism in case of CB is mostly dependent on the stability of the web post rather than material weakening itself. From this test conditions, a critical temperature may be considered at the point when the beam's deflection begins to gradually increase after 10–12 minutes min heating when the temperature on the steel web reaches 550–600 °C (Fig. 9).

(a) Specimen after fire test

(b) Beam1

(c) beam2

(d) beam3

~~Fig 9~~Fig. 9 Bending failure combined post web buckling in all beams.

alt-text: Fig. 9

~~4.~~4 C~~ONCLUSIONS~~onclusions

Structural fire tests were conducted on the unprotected composite cellular beams and the results can be summarized as followings:

1. The furnace having outer frame to give an axial restrain condition to the test beam was developed which enables to modify its restrained stiffness through bracing the member.

2. The temperature profile between 2 types of beam having different slab decking shapes were different at the top flange and upper web as concrete volume mostly influences at the early stage of standard fire.

3. Under the controlled load and restrain conditions, thermal behaviour was followed by beginning of structural yield at 450~~o~~ °C of the steel web post.

4. Results obtained on displacement and strain for beam and restrain frame member show a change of axial force including large deflection of the beam.

5. Under the effect of axial restraint, most beams under investigation experience catenary action at the later heating stage. The axial restraints enable these beams to survive very high temperatures without collapse.

6. Lesser effective depth in case of MD60 as compared to MD50, is compensated for by the presence of double shear connectors and Fig~~ure.~~ 7 demonstrates the similarity of stiffness in both beam types.

Simplified approach method for deflection calculation of composite cellular restrained beams is under consideration.

Parametric study is in progress using the finite element analysis to investigate the effects of slenderness, ratio, type connections and different axial load applications.

ACKNOWLEDGMENTcknowledgment

Acknowledgments to the EPSRC of sponsoring the project and Fisher Ltd. in Northern Ireland for building the surrounding steel frame.

REFERENCESeferences

[1] Interpretative Document No. 2. Essential Requirement on Safety in Case of fire, October 1993, Commission of European Community.

[2] Structural Fire Engineering: Investigation of Broadgate Phase 8 Fire, 1991, Steel Construction Institute.

[3] P.F. Johnson, International developments in fire engineering of steel structures, *J. Constr. Steel Res.* **46**, 1998, 1–3.

[4] C GC.G. Bailey, G.MG.M. Newman and W.I. Simms, Design of Steel Framed Buildings withou Applied Fire Protection. SCI Publication 186, 1999, The Steel Construction Institute (SCI), ISBN 1 85942 062 1.

[5] C.G. Baily, T. Lennon and D.B. Moore, The behavior of full-scale steel-framed building subjected to compartment fires, *The Structural Engineer* **77** (8), 1999, 15–21.

[6] AA. Nadjai, CC. Bailey, OO. Vassart, S. Han, W. I.W.I. Simms, M. Hawes, B. Zhao and J.-M. Franssen, Full -scale fire test on a composite floor slab incorporating long span cellular steel beams, *Journal of The Structural Engineer, London* **Vol. 89** (21), November 2011.

[7] J.A. El-Rimawi, I.W. Burgess and R.J. Plank, Studies of the behavior of steel subframes with semi-rigid connections in fire, *Journal of Constructional Steel Research J. Constr. Steel Res.* **49**, 1999, 83–98.

[8] T. Liu, M. Fahad and J. Davies, Experimental investigation of behaviour of axially restrained steel beams in fire, *J. Constr. Steel Res.* **58**, 2002, 1211–1230, 2002.

[9] M. Wong, Modeling of axial restraints for limiting temperature calculation of steel members in fire, *J. Constr. Steel Res.* **61**, 2005, 675–687, 2005.

[10] G. Li, P. Wang and S. Jiang, Non-linear finite element analysis of axially restrained steel beams at elevated temperatures in a fire, *J. Constr. Steel Res.* **63**, 2007, 1175–1183, 2007.

[11] M. Dwaikat and V. Kodur, A performance based methodology for fire design of restrained steel beams, *J. Constr. Steel Res.* **67**, 2011, 510–524, 2011.

[12] A. Nadjai, O. Vassart, F. Ali, D. Talamona, A. Allam and M. Hawes, Performance of cellular composite floor beams at elevated temperatures, *Fire Saf. J.* **42** (6–7), 2007, 489–497, September–October, 2007.

[13] El-Hadi Naili, Ali Nadjai, Sanghoon Han, Faris Ali and Seng-Kwan Choi, Experimental and Nnumerical Mmodelling of Ccellular Bbeams with Ccircular and Eelongated Wweb Ooopenings at Eelevated Ttemperatures, *Structural Fire Engineering* **2** (4), 2011, 289–300.

[14] O. Vassart, C. Bailey, G. Bihina, M. Hawes, A. Nadjai, C. Peigneux, W.I. Simms and J.M. Franssen, “Parametrical Study on the Behaviour of Steel and Composite Cellular Beams Under Fire Conditions”, 6th SiF10, Michigan, USA, 2-–4 June, 2010, ISBN 978-1-60595-027-32010, 349–357.

[15] BSI, Eurocode 3: design of steel structures — Ppar 1–2: general rules — Sstructural fire design, *CEN* 2005, 2005. EN 1993-1-2:2005(E).

[16] BSI, Eurocode 4: design of composite steel and concrete structures — Ppar 1–2: general rules — Sstructural fire design, *CEN* 2005, 2005. EN 1994-1-2:2005(E).

[17] The Steel Construction Institute, Design of Composite Beams With Large Openings for Services, 2005, SCI Publication, 510–524, 2005, Document RT959.

Queries and Answers

Query:

Your article is registered as a regular item and is being processed for inclusion in a regular issue of the journal. If this is NOT correct and your article belongs to a Special Issue/Collection please contact b.mahesh@elsevier.com immediately prior to returning your corrections.

Answer: Yes

Query:

Please confirm that given names and surnames have been identified correctly and are presented in the desired order, and please carefully verify the spelling of all authors’ names.

Answer: Yes

Query:

The author names have been tagged as given names and surnames (surnames are highlighted in teal color). Please confirm if they have been identified correctly.

Answer: Yes

Query:

The country name "UK" has been inserted for the authors’ affiliation. Please check, and correct if necessary.

Answer: correct

Query:

"Fig. 9" was not cited in the text. Hence, a dummy citation was added here. Please check for proper placement and amend as necessary.

Answer: fine

Query:

Please check captured author names in this ref. item if correct and amend as necessary.

Answer: correct